

# Spatial motion of the magnetic avalanches associated to the CO-AFM to CD-FM transition in $\text{La}_{0.225}\text{Pr}_{0.40}\text{Ca}_{0.375}\text{MnO}_3$ manganite

A. Hernández-Mínguez,<sup>1</sup> F. Macià,<sup>1</sup> J. M. Hernandez,<sup>1</sup> G. Abril,<sup>1</sup> A. García-Santiago,<sup>1</sup> J. Tejada,<sup>1</sup> and F. Parisi<sup>2</sup>

<sup>1</sup>*Departament de Física Fonamental, Facultat de Física, Universitat de Barcelona  
Avda. Diagonal 647, Planta 4, Edifici nou, 08028 Barcelona, Spain*

<sup>2</sup>*Departamento de Física. Comisión Nacional de Energía Atómica and Escuela de Ciencia y Tecnología,  
UNSAM, Av. Gral Paz 1499 (1650) San Martín. Buenos Aires. Argentina.*

(Dated: November 24, 2021)

Very fast magnetic avalanches in (La, Pr)-based manganites are the signature of a phase transition from an insulating blocked charge-ordered (CO-AFM) state to a charge delocalized ferromagnetic (CD-FM) state. We report here the experimental observation that this transition does not occur neither simultaneously nor randomly in the whole sample but there is instead a spatial propagation with a velocity of the order of tens of m/s. Our results show that avalanches are originated in the inside of the sample, move to the outside and occur at values of the applied magnetic field that depend on the CD-FM fraction in the sample. Moreover, a change in the gradient of the magnetic field along the sample shifts the point where the avalanches are ignited.

The study of the coexistence of the two well segregated charge-delocalized ferromagnetic (CD-FM) and charge-ordered antiferromagnetic (CO-AFM) phases in manganites, as well as the influence of the applied magnetic field on the occurrence of the magnetic avalanches accompanying the transition from the CO-AFM phase to the CD-FM phase has nowadays a resurgent interest driven by the unusual (but not uncommon) interplay between static and dynamic properties of the phase separated (PS) state.<sup>1,2,3</sup> Phase separation can appear near the boundary of a first order phase transition (FOPT).<sup>4</sup> In disordered-free magnetic systems the FOPT occurs at a sharply-defined line in the magnetic field-temperature ( $H - T$ ) space. Quenched impurities can lead, under certain circumstances, to the spread of the local transition temperatures (where local means over length scales of the order of the correlation length) leading to the appearance of clustered states with the consequent rounding of the FOPT.<sup>5</sup> The phase separation observed in manganites seems to belong to this last class of systems, being the PS state the true equilibrium state of the system in the vicinity of the FOPT,<sup>6,7</sup> and not just the result of supercooling or superheating of the system. It has been shown<sup>8</sup> that the response of the system within the PS state is governed by a hierarchical cooperative dynamics, with state-dependent energy barriers which diverge as the system approaches equilibrium. This slow growing dynamics, which resembles that of glass-like systems, has given place to the construction of phase diagrams of manganites focused on the dynamic properties of the PS state, with regions of the phase diagrams named as "frozen" or "dynamic" PS<sup>8</sup> "strain glass" or "strain liquid",<sup>9</sup> and the determination of state-dependent blocking or freezing temperatures.<sup>8,10</sup> These kinds of processes are not exclusive of PS manganites, but are also observed in other systems displaying magnetic FOPT.<sup>11,12</sup>

Direct evidences of micrometer phase coexistence in manganites at intermediate temperatures was obtained through electron microscopy<sup>13,14</sup> and magnetic force mi-

croscopy (MFM).<sup>15</sup> A major goal in the description of the low temperature behavior of the PS manganite  $\text{La}_{5/8-y}\text{Pr}_y\text{Ca}_{3/8}\text{MnO}_3$  [LPCM( $y$ ),  $y = 3/8$ ] was achieved recently by Wu *et al.*<sup>2</sup> Using a MFM technique they were able to "photograph" the isothermal evolution of the system as  $H$  varies (a metamagnetic transition), and the evolution at fixed  $H$  when  $T$  increases (the "glass" transition) at the micrometer scale, giving direct evidence of the growing process of the CD-FM phase against the CO-AFM. They conclude, in agreement with the thermodynamic consideration presented in Ref. 10, that the low temperature state accessible after cooling the sample in zero magnetic field could be associated with the supercooled state of the CO-AFM to CD-FM FOPT, the kinetics of the transformation being influenced by accommodation strain between the coexisting phases. The results presented in Ref. 2 were obtained at temperatures above 6 K. Below this temperature the metamagnetic transition between the frozen CO-AFM state and the equilibrium CD-FM phase does not occur in a continuous way,<sup>16,17</sup> at least in the time scale of the MFM experiments (seconds), but it occurs sharply at fields above 2 T, presumably in milliseconds.

In this work we present the study of the dynamics of the CO-AFM to the CD-FM FOPT in LPCM(0.4) below 6 K, and its spatial evolution. A polycrystalline sample of composition  $\text{La}_{0.225}\text{Pr}_{0.40}\text{Ca}_{0.375}\text{MnO}_3$  and dimensions  $2 \times 2 \times 5 \text{ mm}^3$  was used. All magnetic measurements were performed placing the sample inside a commercial Superconducting Quantum Interference Device magnetometer. The sample was first characterized by measuring the temperature and magnetic field dependences of the magnetization. Figure 1 shows that, as  $T$  decreases, the sample experiences a transition from a paramagnetic to a CO-AFM state at  $T_{CO} = 220 \text{ K}$ . A short peak at 190 K reveals the formation of small ferromagnetic clusters before a more robust ferromagnetic transition appears at a lower temperature ( $T_C = 70 \text{ K}$  on cooling,  $T_C = 90 \text{ K}$  on warming). Finally, at  $T_B = 25 \text{ K}$

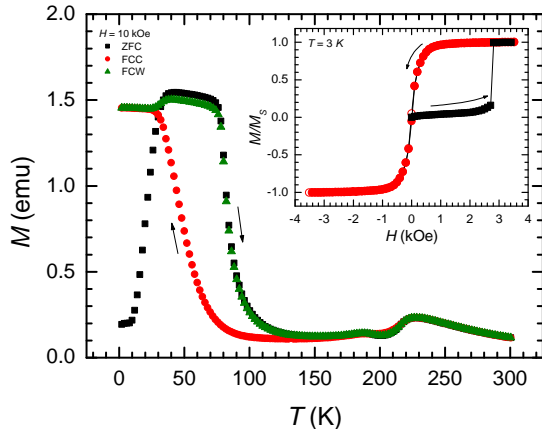


FIG. 1: Temperature dependence of the zero-field cooled (squares), field-cooled on cooling (circles) and field-cooled on warming (triangles) magnetization of  $\text{La}_{0.225}\text{Pr}_{0.4}\text{Ca}_{0.375}\text{MnO}_3$ , measured for a magnetic field of 10 kOe. The inset shows the field dependence of the magnetization with respect to the saturation value,  $M_s$ , at 3 K. Squares correspond to the first magnetization curve, whereas circles show the magnetic measurements from 35 kOe to -35 kOe and back to 35 kOe.

the blocking temperature associated to the energy barriers between the two phases is clearly seen. The inset in Fig. 1 shows the isothermal magnetization curve measured at 3 K. At the first magnetization curve (squares) a magnetic avalanche was detected at 28 kOe, being the final magnetization the saturation value,  $M_s$ , which corresponds to the case of having only the ferromagnetic phase. We then kept the temperature constant and measured, immediately after, a  $M(H)$  going from 35 kOe down to -35 kOe and back to 35 kOe. This hysteresis cycle shows that the ferromagnetic state has neither remanence nor coercivity and, consequently, there are not time dependent phenomena. This point has been further verified by measuring the constancy of the magnetization after fast changes of the magnetic field. All these results are in full agreement with those previously reported for similar PS manganites.<sup>16</sup>

In Fig. 2 we show isothermal  $M(H)$  curves registered at several temperatures comprised between 3 and 5 K after zero-field cooling the sample. Magnetic avalanches are turned on due to the interplay between the local increase of the FM fraction and the heat released in this microscopic transformation.<sup>16</sup> To avoid the ignition of these avalanches, we increased the number of points that were measured at the same interval of applied magnetic field with respect to the hysteresis curve at the inset of Fig. 1. As each point takes several seconds to be measured, this reduces the average sweep rate of the applied magnetic field, allowing the sample to thermalize and

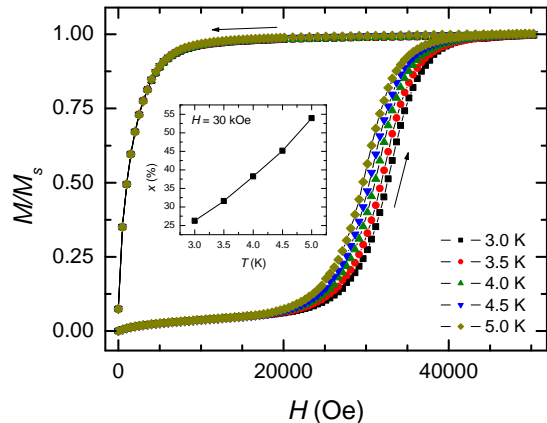


FIG. 2: Isothermal magnetization curves registered at several temperatures between 3 K and 5 K after zero field cooling the sample. The inset shows the temperature dependence of the ferromagnetic phase fraction,  $x$ , for an applied magnetic field of 30 kOe.

making therefore possible to register the  $M$  values of the PS state at many magnetic fields and temperatures where otherwise the sample would have already transited to the CD-FM state. The data of Fig. 2 show that first magnetization curves for field values smaller than 20 kOe coincide, indicating that the FM phase fraction,  $x$ , is nearly the same at all temperatures between 3 and 5 K. The value of  $x$  through out the first magnetization curve can be estimated, at each temperature and magnetic field, from the ratio between  $M$  and  $M_s$ . This definition is no longer valid once  $M_s$  has been achieved, due to the fact that, from then on, all the sample is in the CD-FM state as long as it is not heated and zero-field cooled again. According to this definition, a value of  $x$  smaller than 8% was estimated at 20 kOe. For magnetic fields larger than 20 kOe, there is, however, a separation between the different first magnetization curves indicating that the FM phase fraction depends on both the temperature and the magnetic field. Time dependent phenomena occur in this regime of values of  $T$  and  $H$  indicating that the phase separation is a dynamic process which may be characterized by a barrier height  $U(H, T)$  that separates the CD-FM and the CO-AFM states. The changes in  $x$  are therefore due to thermal transitions above this barrier height. The temperature dependence of  $x$  for 30 kOe is given in the inset of Fig. 2. These values of  $x$  correspond, therefore, to the blocked phase fraction compatible with the time scale of the experiment, that in this case is of the order of seconds.

In the next we will describe the experiments and results when local magnetic measurements are used to study the magnetic avalanches.<sup>18</sup> Figure 3a shows the experimental setup. The sample was placed inside a plastic tube

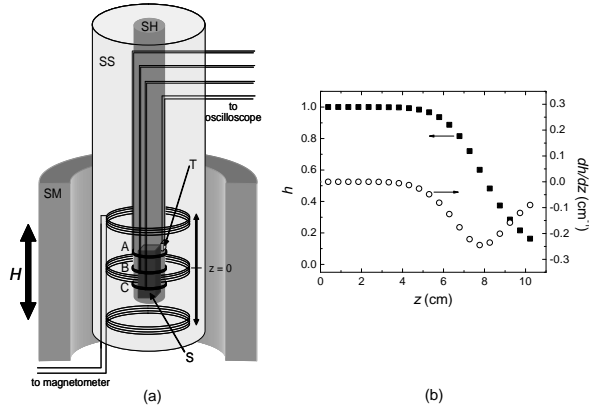


FIG. 3: Experimental setup. (a) The sample (S) is mounted on a sample holder (SH) with three detection coils (A, B and C) and one thermometer (T). This ensemble is introduced in the sample space (SS) of a commercial magnetometer and centered in the superconducting magnet (SM) that applies the magnetic field. The center of the SM is taken as  $z = 0$ . (b) Reduced applied magnetic field (solid squares),  $h(z) = H(z)/H_{max}$  ( $H_{max} = H(z = 0)$ ), and the numerical derivative of such magnitude (open circles),  $dh/dz(z)$ .

and three coils of 4 turns each were wound around the tube, one in the center (coil B) and two at the two edges of the sample (coils A and C, respectively). In Fig. 3b we show the spatial dependence of the reduced magnetic field,  $h = H(z)/H_{max}$ , defined as the ratio between the applied magnetic field value at the position  $z$ ,  $H(z)$ , and the nominal value of the magnetic field applied at the center of the superconducting magnet,  $H_{max}$ . By placing the sample in different positions along the  $z$  axis of the cryostat we may change the field gradient acting along one of the dimensions, as it can be seen in Fig. 3b from the curve of the numerical derivative of the reduced magnetic field,  $dh/dz$ . In these experiments we placed the sample so that the so-called  $z$  direction corresponded to the longest dimension of the sample (see Fig. 3a).

Figure 4 shows the voltages detected by the three coils, which are proportional to the variation of magnetization as a function of time,  $dM/dt$ .  $t = 0$  corresponds to the instant when the avalanche does start and so the three coils detect a non-zero voltage value. These experiments were performed at temperatures comprised between 3 and 5 K, when the sample was centered at  $z = 0$ . As we could only monitorize two signals simultaneously, we repeated the experiment at each temperature several times, registering two different coils each time. The results turned to be highly reproducible and deterministic in this temperature range, so we used the signal detected by coil B to synchronize the signals of all three coils. From Fig. 4 we conclude that the ignition process of the avalanche occurs systematically in the interior of the sample and then moves to the outside. The velocity of propagation of the transformation front can be roughly estimated as

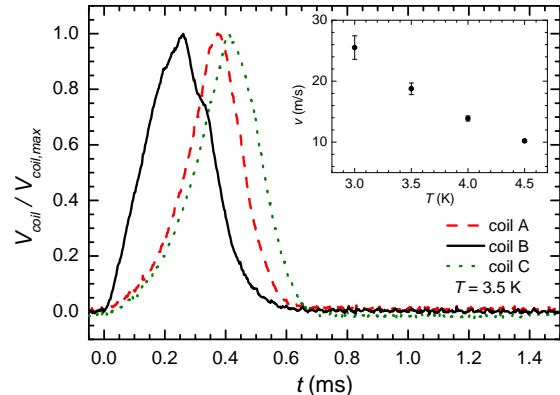


FIG. 4: Time variation of the magnetization as detected by coils A (dashed line), B (solid line) and C (dotted line) at 3.5 K. These three signals have been normalized with respect to their maximum values. The inset shows the propagation velocity of the phase transformation front along the sample as a function of temperature.

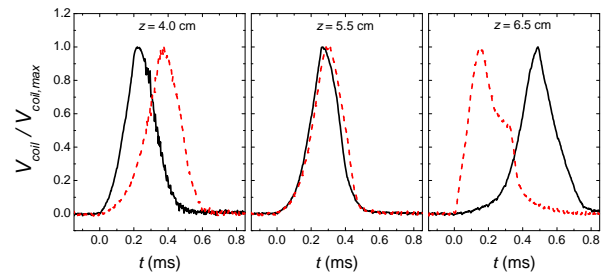


FIG. 5: Time evolution of the voltages detected by coils 1 (solid line) and 2 (dashed line) for different locations of the sample. From left to right,  $z = 4.0$  cm (left panel),  $z = 5.5$  cm (central panel), and  $z = 6.5$  cm (right panel). All signals have been normalized to their maximum values. As  $z$  goes up and the gradient of the applied magnetic field increases, the time sequence of the signal registered by the two detection coils is reversed. The experiment was performed at 3 K.

$v = L/\Delta t$ , where  $L$  is the length of the sample,  $\Delta t$  is defined as  $\Delta t = (t_A - t_B) + (t_C - t_B)$ , and  $t_A$ ,  $t_B$  and  $t_C$  correspond to the times when the signal detected respectively by coils A, B and C is maximum. The thermal dependence of this velocity is shown in the inset of Fig. 4, according to which the average value of  $v$  is about 20 m/s at 3.5 K. As  $T$  and  $x$  are strongly correlated, the velocity of the avalanche also depends on the value of  $x$  when the abrupt phase transition is ignited.

The results shown in Fig. 4 correspond to the case when the applied magnetic field is uniform along the sample. We have also performed experiments shifting the position of the sample along the  $z$  axis. In these cases

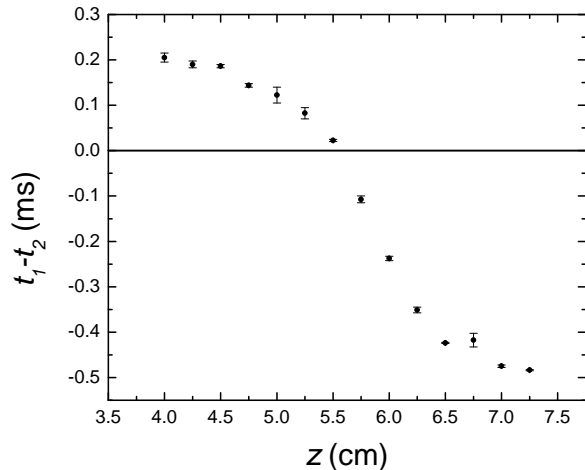


FIG. 6: Variation of the time difference between the maxima of the signal of the two coils,  $t_1 - t_2$ , with respect to  $z$ . The avalanches were ignited at 3.5 K.

the sample suffers the effect of the field and its gradient in such a way that we can obtain variations of the magnetic field along the longest dimension up to a 10% of the maximum value of  $H$  applied. In this case we have used two new detection coils, named 1 and 2, located at the positions where coils A and C previously were. Figure 5 shows the voltages detected by these coils as a function of time for three different positions along the  $z$  direction. Considering that the variation of magnetic field between the two edges of the polycrystal can be roughly estimated as  $\Delta H \sim H_{max} \cdot dh/dz \cdot L$ , where  $L$  is the length of the sample,  $H_{max} \sim 28$  kOe and taking  $dh/dz$  from Fig. 3b, values of  $\Delta H \sim 100, 800$ , and  $2000$  Oe can be obtained at  $z = 4.0, 5.5$  and  $6.5$  cm. The time sequence of the peaks

measured by the detection coils at Fig. 5 shows that the presence of a field gradient affects dramatically the origin and propagation of the abrupt phase transition along the sample. This is more clearly seen at Fig. 6, where we have plotted the time difference between the maxima of the signals in the two coils,  $t_1 - t_2$ , as a function of  $z$ . The sign change in this magnitude reflects that, as the strength of the field gradient increases, the local magnetic field at different points in the sample varies and thus the distribution of energy barriers  $U(H)$  between the AFM and FM phases along the sample is different from that in the case of a homogeneous applied magnetic field. As a consequence, the place of the sample where the abrupt phase transition begins must shift, leading to changes in the signal measured by the detection coils.

In conclusion we have demonstrated that the magnetic avalanches associated to the transition from the CO-AFM metastable state into the CD-FM metallic state by the influence of the applied magnetic field correspond to a phase transformation mechanism that moves along the sample, being ignited in the inside and propagating to the edges. This mechanism reflects, at macroscopic scales, the same physics showed<sup>2</sup> at microscopic ones: when the applied field overcomes certain temperature- and state-dependent threshold value the system becomes unblocked, inducing the growth of the CD-FM phase against the unstable CO-AFM phase. We have also shown that by applying a magnetic field gradient it is possible to change the place in the sample where this threshold is overcome, allowing to modify the position where the avalanche is ignited.

This work was supported by contract MAT2005-06162 from the Spanish Ministerio de Educación y Ciencia (MEyC). A. H.-M. and F. M. thank the MEyC for a research grant. J. M. H. thanks the MEyC and Universitat de Barcelona for a Ramón y Cajal research contract. The authors thank Gabriela Leyva for preparing the sample.

<sup>1</sup> N. Mathur, *Nature Materials* **5**, 849 (2006).  
<sup>2</sup> W. Wu, C. Israel, N. Hur, S. Park, S.-W. Cheong, and A. de Lozanne, *Nature Materials* **5**, 881 (2006).  
<sup>3</sup> E. Dagotto, *Science* **309**, 257 (2005).  
<sup>4</sup> E. Dagotto, *New J. Phys.* **7**, 67 (2005).  
<sup>5</sup> Y. Imry and M. Wortis, *Phys. Rev. B* **19**, 3580 (1979).  
<sup>6</sup> A. Moreo, M. Mayr, A. Feiguin, S. Yunoki, and E. Dagotto, *Phys. Rev. Lett.* **84**, 5568 (2000).  
<sup>7</sup> P. Levy, F. Parisi, L. Granja, E. Indelicato, and G. Polla, *Phys. Rev. Lett.* **89**, 137001 (2002).  
<sup>8</sup> L. Ghivelder and F. Parisi, *Phys. Rev. B* **71**, 184425 (2005).  
<sup>9</sup> P. A. Sharma, S. B. Kim, T. Y. Koo, S. Guha, and S.-W. Cheong, *Phys. Rev. B* **71**, 224416 (2005).  
<sup>10</sup> J. Sacanell, F. Parisi, J. C. P. Campoy, and L. Ghivelder, *Phys. Rev. B* **73**, 014403 (2006).  
<sup>11</sup> K. Kumar, A. K. Pramanik, A. Banerjee, P. Chaddah, S. B. Roy, S. Park, C. L. Zhang, and S.-W. Cheong, *Phys. Rev. B* **73**, 184435 (2006).

<sup>12</sup> M. Chattopadhyay, S. B. Roy, and P. Chaddah, *Phys. Rev. B* **72**, 180401(R) (2005).  
<sup>13</sup> M. Uehara, S. Mori, C. Chen, and S.-W. Cheong, *Nature* **399**, 560 (1999).  
<sup>14</sup> Y. Murakami, J. H. Yoo, D. Shindo, T. Atou, and M. Kikuchi, *Nature* **423**, 965 (2003).  
<sup>15</sup> L. Zhang, C. Israel, A. Biswas, R. L. Greene, and A. de Lozanne, *Science* **298** (2003).  
<sup>16</sup> L. Ghivelder, R. S. Freitas, M. G. das Virgens, M. A. Continentino, H. Martinho, L. Granja, M. Quintero, G. Leyva, P. Levy, and F. Parisi, *Phys. Rev. B* **69**, 214414 (2004).  
<sup>17</sup> R. Mahendiran, A. Maignan, S. Hébert, C. Martin, M. Hervieu, B. Raveau, J. F. Mitchell, and P. Schiffer, *Phys. Rev. Lett.* **89**, 286602 (2002).  
<sup>18</sup> A. Hernández-Mínguez, F. Macià, J. M. Hernandez, J. Tejada, L. H. He, and F. F. Wang, *Europhys. Lett.* **75**, 811 (2006).